



Title	Validation Study on the Accuracy of Echocardiographic Measurements of Right Ventricular Systolic Function in Pulmonary Hypertension
Author(s)	Sato, Takahiro; Tsujino, Ichizo; Ohira, Hiroshi; Oyama-Manabe, Noriko; Yamada, Asuka; Ito, Yoichi M.; Goto, Chisa; Watanabe, Taku; Sakaue, Shinji; Nishimura, Masaharu
Citation	Journal of the American Society of Echocardiography, 25(3), 280-286 https://doi.org/10.1016/j.echo.2011.12.012
Issue Date	2012-03
Doc URL	http://hdl.handle.net/2115/48647
Type	article (author version)
File Information	JASE25-3_280-286.pdf



[Instructions for use](#)

Validation study on the accuracy of echocardiographic measurements of right ventricular systolic function in pulmonary hypertension

Takahiro Sato, M.D.^a, Ichizo Tsujino, M.D., Ph.D.^a, Hiroshi Ohira, M.D., Ph.D.^a,
Noriko Oyama-Manabe, M.D., Ph.D.^b, Asuka Yamada, M.D.^a, Yoichi M. Ito, Ph.D.^c, Chisa Goto,
M.D.^a, Taku Watanabe, M.D.^a, Shinji Sakaue, M.D., Ph.D.^d,
Masaharu Nishimura, M.D., Ph.D.^d

^aFirst Department of Medicine and ^bDepartment of Diagnostic and Interventional Radiology,
Hokkaido University Hospital, ^cDepartment of Biostatistics, Hokkaido University Graduate School
of Medicine, ^dFirst Department of Medicine, Hokkaido University School of Medicine, Sapporo,
Japan

Short title: Assessment of right ventricular function in PH

Name of grant(s): None to report

Corresponding author: Ichizo Tsujino M.D., Ph.D.
First Department of Medicine, Hokkaido University Hospital,
North 14, West 5, Kita-ku, Sapporo 060-8648, Japan.
Tel: +81-11-706-5911, FAX: +81-11-706-7899
E-mail: itsujino@med.hokudai.ac.jp

Abstract word count: 221 words, Main document word count: 2692

Number of tables: 2, Number of figures: 4

Abstract

Background: Accuracy of echocardiographic parameters of right ventricular (RV) function has not been sufficiently validated in patients with pulmonary hypertension (PH). We attempted to evaluate whether echocardiographic measurements reliably reflect RV systolic function in PH using cardiac magnetic resonance imaging (CMRI)-derived RV ejection fraction (EF) as a gold standard.

Materials and Methods: A total of thirty-seven consecutive patients with PH, 20 with pulmonary arterial hypertension, 12 with chronic thromboembolic pulmonary hypertension, and 5 others, were prospectively studied. All patients underwent echocardiography, CMRI and right heart catheterization within a 1-week interval. Associations between 5 echocardiography-derived parameters of RV systolic function and CMRI-derived RVEF were evaluated.

Results: All 5 echocardiography-derived parameters were significantly correlated with CMRI-derived RVEF (%RV fractional shortening: $r=0.48$, $p=0.0011$; %RV area change: $r=0.40$, $p=0.0083$; tricuspid annular plane systolic excursion (TAPSE): $r=0.86$, $p<0.0001$, RV myocardial performance index: $r=-0.59$, $p<0.0001$; and systolic lateral tricuspid annular motion velocity (TV_{lat}): $r=0.63$, $p<0.0001$). When compared with the other indices, TAPSE exhibited the highest correlation coefficient. Of the 5 echocardiographic measurements, only TAPSE significantly predicted CMRI-derived RVEF in multiple regression analysis ($p<0.0001$). Intra- and interobserver reproducibility was favorable for all 5 indices, and for TAPSE and TV_{lat} was particularly high.

Conclusion: Echocardiographic measurements are promising noninvasive indices of RV systolic function in patients with PH. In particular, TAPSE is superior to other indices in accuracy.

Keywords: pulmonary hypertension, echocardiography, right ventricular systolic function, tricuspid annular plane systolic excursion

Introduction

Pulmonary hypertension (PH) is defined as a mean pulmonary arterial pressure (PAP) greater than 25 mmHg at rest (1). PH imposes pressure overload onto the right ventricle through elevated PAP, which can cause premature death in advanced cases. Precise evaluation of right ventricular (RV) function is thus critical in the management of PH, although complex RV chamber geometry limits accurate assessment of RV function.

Recently, however, progress in cardiac magnetic resonance imaging (CMRI) has enabled accurate calculation of RV ejection fraction (EF) (RVEF) in PH patients (2-3). However, quantitative assessment of RV function using CMRI requires a dedicated program and expertise, which limits its widespread application and use.

In contrast, echocardiography is a convenient and readily accessible tool for evaluation of RV function. To date, several echocardiographic parameters have been introduced for assessment of RV function (4-11). However, their accuracy has been tested mostly in patients with non-PH diseases or in control subjects (6, 12-17). Moreover, a gold standard with sufficient accuracy was not applied in most studies (6, 12, 17-18), hampering their broad use as reliable indices of RV function. In addition, no studies have systematically compared the accuracy and reproducibility of these echocardiographic indices. Accordingly, in the present study we attempted to validate whether currently available echocardiographic measurements reliably reflect RV systolic function in PH

patients using CMRI-derived RVEF as a gold standard. We also sought to determine which echocardiographic measurement is superior to other indices in terms of accuracy.

Materials and Methods

Patients with PH were prospectively enrolled between April 2010 and February 2011. A mean PAP of ≥ 25 mmHg and pulmonary wedge pressure of ≤ 15 mmHg evaluated by right heart catheterization (RHC) were used as entry criteria (1). Exclusion criteria were: 1) inability of obtaining/analyzing images of CMRI or echocardiography for any reason, 2) comorbid left heart disease(s) that may affect RV geometry and function, and 3) signs/symptoms indicative of an unstable condition of PH. All enrollees underwent echocardiography, CMRI and RHC within one week.

Echocardiograms were obtained using Vivid q (GE Healthcare, Milwaukee, WI, USA), and images were analyzed off-line after the procedure. A two-dimensional apical 4-chamber view was used to obtain %RV fractional shortening (%RVFS) and %RV area change. An established method was used to calculate both indices (19). Briefly, %RVFS was obtained by calculating regional changes of the distance from the interventricular septum to the RV free wall at the mid RV level between end-diastole and end-systole (Fig. 1A). %RV area change was calculated by dividing the difference in RV area between the end-diastolic and end-systolic phases by end-diastolic RV area.

The endomyocardial contour was traced from the tricuspid annulus along the free wall to the apex, then back to the annulus, along the interventricular septum. Trabeculation, tricuspid leaflets and chords were included in the chamber (Fig. 1B). M-mode images were used to obtain tricuspid annular plane systolic excursion (TAPSE), as has been reported previously (6-7). In short, the M-mode cursor was oriented to the junction of tricuspid valve plane with the RV free wall, and the total displacement of the tricuspid annulus from end-diastole to end-systole was measured (Fig. 1C). The RV myocardial performance index (RV MPI) was calculated by subtracting RV outflow velocity time (b) from the interval between cessation and onset of tricuspid flow velocity (a), and the difference (a-b) was divided by RV outflow velocity time [(a-b)/b] (Fig. 1D) (8). Pulsed-wave tissue Doppler imaging (TDI) of systolic lateral tricuspid annular motion velocity (TV_{lat}) was obtained from the apical 4-chamber view using a sampling gate of 2-4 mm and a sweep velocity of 100–150 mm/s. An ultrasound cursor was carefully placed parallel to the direction of the tricuspid annular motion, and TV_{lat} was measured in the TDI mode using minimal gain and a reduced high pass filter, minimizing signals from noise (Fig. 1E) (20). Image acquisition and analysis were performed by a single experienced cardiologist unaware of the CMRI measurements (T.S.).

CMRI studies were performed on a 1.5-Tesla Philips Achieva MRI system (Philips Medical Systems, Best, The Netherlands) with Master gradients (maximum gradient amplitude 33 mT/m, maximum slew rate 100 mT/m/ms). Imaging was performed with subjects in the supine

position using a five-element cardiac phased-array coil with breath-holding in expiration, and with a vector-cardiographic method for ECG-gating. Localizing scans were followed by breath-hold cine imaging in the axial orientation. From the coronal localizing images that demonstrated gross cardiac anatomy, a transverse stack of slices was planned to cover the heart from a level just below the diaphragm to the bronchial bifurcation, covering the heart in diastole. A total of 12 axial slices were acquired using an SSFP pulse sequence (TR=2.8 ms, TE=1.4 ms, flip angle=60, acquisition matrix=192 × 256, field of view=380 mm, slice thickness=10 mm, 0 mm inter-slice gap, 20 phases/cardiac cycle).

Image analysis of right and left ventricles was performed off-line using commercially available analysis software (Extended MR Work Space: ver. 2.6.3, Philips Medical Systems, Amsterdam, The Netherlands). The contour tracing was aided by reviewing the multiple phase scans in the movie mode. In the axial data sets, the endocardial contours of the right ventricle were traced manually at the first phase and at the two phases in the middle of the cardiac cycle with the smallest volumes. The workstation selected the first phase of each slice as end-diastole, and the smaller of the two middle phases as end-systole. The contours were traced starting at the most apical slice and finishing with the uppermost slice. The RV contours were traced up to the tricuspid valve and closed by a straight line across the tricuspid valve ring. The uppermost slice was defined as the first slice where a pulmonary cusp could be identified (21). In this uppermost slice, both in end-diastole and in

end-systole, the area of the pulmonary cusp was excluded from the volume. Slices above that level were considered to include the main pulmonary artery and were excluded from the RV volume. The most apical slice was defined as the last slice to contain blood volume. RV and left ventricular (LV) end-diastolic volume (EDV) and end-systolic volumes (ESV) were computed. RV and LV stroke volume (SV) and ejection fraction (EF) were calculated as $SV = EDV - ESV$ and $EF = SV / EDV \times 100\%$, respectively. CMRI analysis was performed by a single experienced radiologist who was unaware of the results of echocardiographic evaluations (N.M.). The same observer (N.M.) repeated the RVEF measurements in 10 randomly selected patients, with at least two weeks between measurements, in order to assess intraobserver variability. A second observer (T.S.) also repeated RVEF measurements of the same 10 patients for assessment of interobserver variability. Bland-Altman analysis and intraclass correlations (ICC) between the two measurements were used to assess the intra- and interobserver reproducibility.

The relationship between echocardiographic measurements and CMRI-derived RVEF was assessed by Pearson's correlation coefficient. Multiple regression analysis was also conducted to examine if any of the 5 echocardiographic measurements were associated with CMRI-derived RVEF in an independent manner. Intraobserver agreement for echocardiographic measurements was assessed by comparing the measurements of repeated analysis in 10 randomly chosen patients (T.S.). This repeated analysis was performed 1 to 3 months after the initial assessment. Interobserver

agreement was assessed using the same patients (n=10) by comparing the results measured by T.S. and by a second, experienced cardiologist (I.T.). The second cardiologist was not aware of either the echocardiographic measurements by the first examiner or of the CMRI measurements. Bland-Altman analysis and ICC between the two measurements were used to assess intra- and interobserver reproducibility.

All statistical analyses were performed using JMP[®] Version 8 (SAS Institute Inc, Cary, NC, USA), and p values less than 0.05 were considered statistically significant. The present study was approved by the ethics committee of the Hokkaido University Graduate School of Medicine, and written informed consent was obtained from all patients.

Results

A total of 39 patients met the entry criteria during the study period, but 2 were excluded due to prespecified exclusion criteria (inability to undergo CMRI due to claustrophobia in 1 patient, and hypertrophic cardiomyopathy in another). Clinical characteristics and CMRI and RHC measurements of the 37 PH patients are summarized in Table 1. Brand-Altman analysis of CMRI-derived RVEF showed high agreement in both intra- and interobserver reproducibility (mean \pm limit of agreement: intraobserver, 0.73 ± 3.3 ; interobserver, -1.5 ± 3.2). ICC of intra- and interobserver reproducibility was 0.99 and 0.98, respectively.

Table 2 shows echocardiographic parameters, and all 5 echocardiography-derived parameters were shown to significantly correlate with CMRI-derived RVEF (%RVFS: $r=0.48$, $p=0.0011$; %RV area change: $r=0.40$, $p=0.0083$; TAPSE: $r=0.86$, $p<0.0001$, RV MPI: $r=-0.59$, $p<0.0001$; TV_{lat} : $r=0.63$, $p<0.0001$). Of these echocardiographic indices, TAPSE exhibited the highest correlation coefficient with RVEF (Fig. 2). In multiple regression analysis, among the 5 echocardiographic measurements, only TAPSE significantly predicted CMRI-derived RVEF (%RVFS, $p=0.12$; %RV area change, $p=0.89$; TAPSE, $p<0.0001$; RV MPI, $p=0.74$; TV_{lat} , $p=0.32$).

Bland-Altman analysis of intraobserver variability of the echocardiographic indices showed small mean differences and limits of agreement (%RVFS $0.1\pm 2.5\%$, %RV area change $2.6\pm 8.4\%$, TAPSE 0.4 ± 2.2 mm, RV MPI -0.01 ± 0.14 , TV_{lat} -0.02 ± 0.49 cm/s (Fig. 3)). ICCs were greater than 0.9 for all 5 measurements (%RV FS 0.95, %RV area change 0.92, TAPSE 0.98, RV MPI 0.95, TV_{lat} 0.99). Regarding interobserver variability, Bland-Altman analysis showed similarly small mean differences and limits of agreement (%RVFS $-0.2\pm 6.0\%$, %RV area change $-2.5\pm 15.8\%$, TAPSE 0.1 ± 2.2 mm, RV MPI -0.00 ± 0.14 , TV_{lat} 0.09 ± 0.49 cm/s (Fig. 4)). ICCs were acceptably high for all measurements, whereas those of only TAPSE and TV_{lat} were 0.9 or higher (%RV FS 0.81, %RV area change 0.63, TAPSE 0.90, RV MPI 0.81, TV_{lat} 0.93).

Discussion

The present study demonstrated that echocardiographic measurements of RV systolic function significantly correlated with CMRI-derived RVEF in PH patients. In particular, TAPSE exhibited the strongest independent correlation with RVEF with sufficient reproducibility. To the best of our knowledge, this study is the first to systematically validate the accuracy of echocardiographic indices of RV systolic function in PH patients using CMRI as a gold standard.

A significant correlation between TAPSE and RV systolic function was demonstrated by Kaul et al. in 1984 (6). Since then, TAPSE has been used as an index of RV systolic function in many publications (6, 13, 15-17, 19, 22). It should be noted, however, that Kaul et al. used patients with ischemic heart disease and healthy controls who had no overt PH. Furthermore, they measured RVEF using radionuclide angiography, a technique with temporal and spatial resolution that is known to be limited. Another report by Ghio et al. documented that TAPSE and echocardiographically-derived %RV area change were significantly associated with RVEF. They recruited only subjects with PH; however, RVEF was indirectly calculated using thermodilution method-derived data (22). We thus believe the significant correlation between TAPSE and RVEF observed in the present study is meaningful in the clinical setting of PH, because we examined only patients with PH, and because we used CMRI, a method that provides improved temporal and spatial resolution.

Significant associations between TV_{lat} and RVEF have also been reported (20, 23). In the

previous reports, however, populations studied were patients with left-sided heart failure, and those with PAH were not or only partially included. In the present study, we examined only PH patients and found a significant correlation between the 2 parameters, which verified the use of TV_{lat} as a reliable parameter of RV systolic function in PH.

Both TAPSE and TV_{lat} are indices that reflect longitudinal RV movement. The right ventricle contracts predominantly along the longitudinal plane rather than the short axis plane in healthy subjects (24). This has not been verified in PH, but still suggests theoretical advantage of these parameters over short-plane indices. This is in contrast with the left ventricle that primarily contracts in the short axis plane. In assessment of LV systolic function, parameters that reflect short-axis movement are predominantly used. Another feature of TAPSE and TV_{lat} is that they can be easily obtained in almost all patients (25). This is because the 2 parameters require an apical 4-chamber window that is available in the vast majority of patients, and also use a simple M-mode and TDI measurement without complex data post-processing. Indeed, ICCs of TAPSE and TV_{lat} are better than the other indices in both intra- and interobserver variability analyses.

Recently, Kind et al. (26) reported a better accuracy of %RVFS as compared to TAPSE in predicting RVEF in PH patients. Between that study and the present study, the patient population and the applied treatment regimens varied. Kind et al. also measured TAPSE by CMRI, but we measured it with echocardiography. In fact, echocardiography has limited ability in visualizing the

lateral wall of ventricles compared with CMRI. This might have produced better accuracy for short-axis indices compared to the longitudinal indices in the study by Kind et al. Further evaluation on more appropriate use of different types of echocardiographic indices is therefore needed.

%RV area change is another widely-used echocardiographic measure of RV systolic function that correlates well with RVEF in various clinical settings (12, 27). However, in the present study, %RV area change correlated only weakly with RVEF. This is, at least partly, due to an enlarged RV cavity and/or hypertrophied RV trabeculae that are likely to hamper accurate assessment of %RV area change. Indeed, %RV area change was not calculated in 3 patients in the present study because a clear 4-chamber view of RV cavity was not obtained in these subjects. This known limitation of echocardiography may have contributed to the poorer accuracy and reproducibility of %RV area change and of RVFS as compared with TAPSE and TV_{1at} .

Correlation of the RV MPI with CMRI-derived RVEF ($r=-0.59$) was not sufficiently strong. This may suggest a limitation of the use of RV MPI as a measure of RV function. However, it should be noted that the RV MPI reveals both systolic and diastolic RV function in patients with PH (8). Furthermore, the RV MPI enables dynamic evaluation of RV function under different loading conditions, which might be a unique advantage of this index over other parameters.

Recently, promising echocardiographic parameters have become available for assessment of RV function in patients with PH, such as real-time three-dimensional echocardiography (28), or

the speckle tracking method which enables evaluation of the global and regional RV systolic function (29). These indices, however, need post hoc off-line analysis by dedicated software unlike the 5 measurements evaluated in the present study. Accuracy, reproducibility, and the clinical relevance of these new parameters will be determined by larger and longer clinical studies.

One limitation of the present study is the inclusion of only a small number of patients. The present study was conducted in a medium-sized single center and, thus, the number of eligible PH patients was limited. However, the statistical power of our study was greater than 0.8 with a significance level of 0.05 (30), given the estimation based on previous studies that the correlation coefficient between CMRI-derived RVEF and echocardiographic parameters was 0.5 or greater (15). Second, echocardiography, CMRI and RHC were not performed simultaneously, which potentially hampers accurate comparison among the evaluations. However, all patients were in a stable clinical condition during the study period without any therapeutic modification. Third, there were 6 patients who had reduced LVEF (<50%), which could have potentially affected TAPSE (31). With regards to this point, additional analysis was conducted and a significant association was found between TAPSE and CMRI-derived RVEF in PH patients without low LVEF ($r=0.77$, $p<0.0001$, $n=31$). Lastly, the present study did not allow for evaluation of the diverse impacts of different disease stages or etiologies of PH on the accuracy of echocardiographic indices. Larger studies with controlled enrollment of patients with different stages and etiologies of PH need to be conducted to

address this issue.

In conclusion, this study demonstrated that echocardiographic measurements are promising noninvasive indices of RV systolic function in patients with PH. In particular, TAPSE is superior to other indices in accuracy. Optimal application of these indices is expected to enable more accurate assessment of cardiac function and thus better management of patients with PH.

Acknowledgement

We are thankful to Dr. Daisuke Ikeda and to Dr. Megumu Ohira for planning the study protocol and interpretation of the obtained data.

References

1. Galie N, Hoeper MM, Humbert M, Torbicki A, Vachiery JL, Barbera JA, et al. Guidelines for the diagnosis and treatment of pulmonary hypertension: The Task Force for the Diagnosis and Treatment of Pulmonary Hypertension of the European Society of Cardiology (ESC) and the European Respiratory Society (ERS), endorsed by the International Society of Heart and Lung Transplantation (ISHLT). *Eur Heart J*. 2009 Oct;30(20):2493-537.
2. McLure LE, Peacock AJ. Cardiac magnetic resonance imaging for the assessment of the heart and pulmonary circulation in pulmonary hypertension. *Eur Respir J*. 2009 Jun;33(6):1454-66.
3. Chin KM, Kingman M, de Lemos JA, Warner JJ, Reimold S, Peshock R, et al. Changes in right ventricular structure and function assessed using cardiac magnetic resonance imaging in bosentan-treated patients with pulmonary arterial hypertension. *Am J Cardiol*. 2008 Jun 1;101(11):1669-72.
4. Rajagopalan N, Simon MA, Shah H, Mathier MA, Lopez-Candales A. Utility of right ventricular tissue Doppler imaging: correlation with right heart catheterization. *Echocardiography*. 2008 Aug;25(7):706-11.
5. Lopez-Candales A, Rajagopalan N, Dohi K, Edelman K, Gulyasy B. Normal range

of mechanical variables in pulmonary hypertension: a tissue Doppler imaging study.

Echocardiography. 2008 Sep;25(8):864-72.

6. Kaul S, Tei C, Hopkins JM, Shah PM. Assessment of right ventricular function using two-dimensional echocardiography. *Am Heart J*. 1984 Mar;107(3):526-31.

7. Forfia PR, Fisher MR, Mathai SC, Houston-Harris T, Hemnes AR, Borlaug BA, et al. Tricuspid annular displacement predicts survival in pulmonary hypertension. *Am J Respir Crit Care Med*. 2006 Nov 1;174(9):1034-41.

8. Tei C, Dujardin KS, Hodge DO, Bailey KR, McGoon MD, Tajik AJ, et al. Doppler echocardiographic index for assessment of global right ventricular function. *J Am Soc Echocardiogr*. 1996 Nov-Dec;9(6):838-47.

9. Wahl A, Praz F, Schwerzmann M, Bonel H, Koestner SC, Hullin R, et al. Assessment of right ventricular systolic function: comparison between cardiac magnetic resonance derived ejection fraction and pulsed-wave tissue Doppler imaging of the tricuspid annulus. *Int J Cardiol*. 2011 Aug 18;151(1):58-62.

10. Brown SB, Raina A, Katz D, Szerlip M, Wiegers SE, Forfia PR. Longitudinal shortening accounts for the majority of right ventricular contraction and improves after pulmonary vasodilator therapy in normal subjects and patients with pulmonary arterial hypertension. *Chest*. 2011 Jul;140(1):27-33.

11. Fukuda Y, Tanaka H, Sugiyama D, Ryo K, Onishi T, Fukuya H, et al. Utility of right ventricular free wall speckle-tracking strain for evaluation of right ventricular performance in patients with pulmonary hypertension. *J Am Soc Echocardiogr.* 2011 Oct;24(10):1101-8.
12. Zimbarra Cabrita I, Ruisanchez C, Dawson D, Grapsa J, North B, Howard LS, et al. Right ventricular function in patients with pulmonary hypertension; the value of myocardial performance index measured by tissue Doppler imaging. *Eur J Echocardiogr.* 2010 Sep;11(8):719-24.
13. Calcuttea A, Chung R, Lindqvist P, Hodson M, Henein MY. Differential right ventricular regional function and the effect of pulmonary hypertension: three-dimensional echo study. *Heart.* 2011 Jun;97(12):1004-11.
14. Wang J, Prakasa K, Bomma C, Tandri H, Dalal D, James C, et al. Comparison of novel echocardiographic parameters of right ventricular function with ejection fraction by cardiac magnetic resonance. *J Am Soc Echocardiogr.* 2007 Sep;20(9):1058-64.
15. Morcos P, Vick GW, 3rd, Sahn DJ, Jerosch-Herold M, Shurman A, Sheehan FH. Correlation of right ventricular ejection fraction and tricuspid annular plane systolic excursion in tetralogy of Fallot by magnetic resonance imaging. *Int J Cardiovasc Imaging.* 2009 Mar;25(3):263-70.

16. Kjaergaard J, Petersen CL, Kjaer A, Schaadt BK, Oh JK, Hassager C. Evaluation of right ventricular volume and function by 2D and 3D echocardiography compared to MRI. *Eur J Echocardiogr.* 2006 Dec;7(6):430-8.
17. Ueti OM, Camargo EE, Ueti Ade A, de Lima-Filho EC, Nogueira EA. Assessment of right ventricular function with Doppler echocardiographic indices derived from tricuspid annular motion: comparison with radionuclide angiography. *Heart.* 2002 Sep;88(3):244-8.
18. Miller D, Farah MG, Liner A, Fox K, Schluchter M, Hoit BD. The relation between quantitative right ventricular ejection fraction and indices of tricuspid annular motion and myocardial performance. *J Am Soc Echocardiogr.* 2004 May;17(5):443-7.
19. Rudski LG, Lai WW, Afilalo J, Hua L, Handschumacher MD, Chandrasekaran K, et al. Guidelines for the echocardiographic assessment of the right heart in adults: a report from the American Society of Echocardiography endorsed by the European Association of Echocardiography, a registered branch of the European Society of Cardiology, and the Canadian Society of Echocardiography. *J Am Soc Echocardiogr.* 2010 Jul;23(7):685-713; quiz 86-8.
20. Wahl A, Praz F, Schwerzmann M, Bonel H, Koestner SC, Hullin R, et al. Assessment of right ventricular systolic function: Comparison between cardiac magnetic resonance derived ejection fraction and pulsed-wave tissue Doppler imaging of the tricuspid

annulus. *Int J Cardiol.* 2010 May 26.

21. Alfakih K, Plein S, Bloomer T, Jones T, Ridgway J, Sivananthan M. Comparison of right ventricular volume measurements between axial and short axis orientation using steady-state free precession magnetic resonance imaging. *J Magn Reson Imaging.* 2003 Jul;18(1):25-32.

22. Ghio S, Raineri C, Scelsi L, Recusani F, D'Armini A M, Piovella F, et al. Usefulness and limits of transthoracic echocardiography in the evaluation of patients with primary and chronic thromboembolic pulmonary hypertension. *J Am Soc Echocardiogr.* 2002 Nov;15(11):1374-80.

23. Meluzin J, Spinarova L, Bakala J, Toman J, Krejci J, Hude P, et al. Pulsed Doppler tissue imaging of the velocity of tricuspid annular systolic motion; a new, rapid, and non-invasive method of evaluating right ventricular systolic function. *Eur Heart J.* 2001 Feb;22(4):340-8.

24. Rushmer RF, Crystal DK, Wagner C. The functional anatomy of ventricular contraction. *Circ Res.* 1953 Mar;1(2):162-70.

25. Alam M, Wardell J, Andersson E, Samad BA, Nordlander R. Characteristics of mitral and tricuspid annular velocities determined by pulsed wave Doppler tissue imaging in healthy subjects. *J Am Soc Echocardiogr.* 1999 Aug;12(8):618-28.

26. Kind T, Mauritz GJ, Marcus JT, van de Veerdonk M, Westerhof N, Vonk-Noordegraaf A. Right ventricular ejection fraction is better reflected by transverse rather than longitudinal wall motion in pulmonary hypertension. *J Cardiovasc Magn Reson.* 2010;12:35.
27. Anavekar NS, Gerson D, Skali H, Kwong RY, Yucel EK, Solomon SD. Two-dimensional assessment of right ventricular function: an echocardiographic-MRI correlative study. *Echocardiography.* 2007 May;24(5):452-6.
28. Grapsa J, O'Regan DP, Pavlopoulos H, Durighel G, Dawson D, Nihoyannopoulos P. Right ventricular remodelling in pulmonary arterial hypertension with three-dimensional echocardiography: comparison with cardiac magnetic resonance imaging. *Eur J Echocardiogr.* 2010 Jan;11(1):64-73.
29. Pirat B, McCulloch ML, Zoghbi WA. Evaluation of global and regional right ventricular systolic function in patients with pulmonary hypertension using a novel speckle tracking method. *Am J Cardiol.* 2006 Sep 1;98(5):699-704.
30. Machin D, Campbell M, Fayers PM, Pinol A. *Sample Size Tables for Clinical Studies, Second Edition*, Malden, MA: Blackwell Science Ltd; 1997. p 168-173
31. Lopez-Candales A, Rajagopalan N, Saxena N, Gulyasy B, Edelman K, Bazaz R. Right ventricular systolic function is not the sole determinant of tricuspid annular motion.

Am J Cardiol. 2006 Oct 1;98(7):973-7.

Table 1. Baseline demographics, and results of magnetic resonance imaging and right heart catheterization

Diagnosis	
Pulmonary arterial hypertension ^{*1}	20
Chronic thromboembolic pulmonary hypertension	12
Other	5
Age (years)	53 ± 15
Male/Female	11/26
WHO functional class	
I	1 (3%)
II	15 (41%)
III	16 (43%)
IV	5 (14%)
Use of pulmonary hypertension-specific vasodilators ^{*2}	
Beraprost	14 (38%)
Bosentan	12 (32%)
Ambrisentan	1 (3%)

Sildenafil	11 (30%)
Tadalafil	1 (3%)
Epoprostenol	4 (11%)
6 minute walk distance ^{*3} (m)	386 ± 117
Brain natriuretic peptide (pg/ml)	218 ± 395

Hemodynamics

Systolic systemic blood pressure (mmHg)	118 ± 20
Diastolic systemic blood pressure (mmHg)	67 ± 12
Pulmonary capillary wedge pressure (mmHg)	8 ± 2
Mean pulmonary artery pressure (mmHg)	39 ± 10
Systolic pulmonary artery pressure (mmHg)	64 ± 20
Diastolic pulmonary artery pressure (mmHg)	24 ± 7
Mean right atrium pressure (mmHg)	6 ± 2
Cardiac index (L/min/m ²) ^{*4}	2.8 ± 0.8
Pulmonary vascular resistance (dyne · s · cm ⁻⁵)	612 ± 271
Mixed venous O ₂ saturation (%) ^{*5}	68 ± 7

Magnetic resonance imaging results

Left ventricular ejection fraction (%)	59 ± 10
--	---------

Left ventricular end diastolic volume (ml)	100 ± 33
Left ventricular end systolic volume (ml)	44 ± 26
Right ventricular ejection fraction (%)	38 ± 11
Right ventricular end diastolic volume (ml)	183 ± 66
Right ventricular end systolic volume (ml)	118 ± 61

Data are presented as mean ± SD.

*1 Idiopathic pulmonary arterial hypertension 8, connective tissue disease-associated

pulmonary arterial hypertension 8, other 4. *2 Pulmonary hypertension-specific drugs were

used in combination in 14 patients (39%). *3 Not performed in 5 patients who were WHO

functional class IV. *4 Mean of at least 3 measurements obtained by thermodilution method. *5

Obtained during oxygen inhalation (0.5-8 l/min) in 7 patients.

Table 2. Echocardiographic features of the pulmonary hypertension patients.

Left ventricular diastolic diameter (mm)	41 ± 6
Left ventricular systolic diameter (mm)	23 ± 6
Left ventricular fractional shortening (%)	43 ± 9
Interventricular septal wall thickness (mm)	8.9 ± 1.6
Left ventricular posterior wall thickness (mm)	8.6 ± 2.1
Diastolic eccentricity index	1.3 ± 0.2
Systolic eccentricity index	1.5 ± 0.4
Left ventricular myocardial performance index	0.41 ± 0.20
Tricuspid regurgitation grade (none/mild/moderate/severe)	4/19/10/4
Tricuspid regurgitation pressure gradient (mmHg) ^{*1}	65 ± 20
Right ventricular fractional shortening (%)	20 ± 8
Right ventricular area change (%) ^{*2}	31 ± 17
Tricuspid annular plane systolic excursion (mm)	19 ± 4
Right ventricular end diastolic area (cm ²)	21 ± 7
Right ventricular end systolic area (cm ²)	15 ± 6
Right ventricular myocardial performance index	0.51 ± 0.23

Lateral tricuspid annular systolic motion velocity (cm/s) 9.3 ± 2.4

Data are presented as mean \pm SD.

*1 Tricuspid regurgitation was not obtained in 4 patients. *2 %RV area change was not obtained in 3 patients due to incomplete image acquisition.

Figure legends

Fig. 1. Representative echocardiographic images of the assessment of right ventricular systolic function

A. %RV fractional shortening $[(a-b)/a \times 100 (\%)]$, B. %RV area change $[(a-b)/a \times 100 (\%)]$, C. Tricuspid annular plane systolic excursion, D. Right ventricular myocardial performance index $[(a-b)/b]$, E. Systolic lateral tricuspid annular motion velocity. See text for further information how these indices were obtained or calculated.

Fig. 2.

Relationships between cardiac magnetic resonance imaging-derived right ventricular ejection fraction and five echocardiographic indices of right ventricular systolic function

All five echocardiography-derived indices of right ventricular systolic function were significantly correlated with cardiac magnetic resonance imaging-derived right ventricular ejection fraction.

Among the echocardiography-derived indices, tricuspid annular plane systolic excursion exhibited the highest correlation coefficient ($r=0.86$) with a p-value of less than 0.0001.

Fig. 3. Bland-Altman analyses between intraobserver measurements of the five

echocardiographic parameters

Solid lines on Bland-Altman plots indicate mean differences; dashed lines indicate limits of agreement. %RVFS, right ventricular fractional shortening; TAPSE, tricuspid annular plane systolic excursion; RV MPI, right ventricular myocardial performance index; TV_{lat} , systolic lateral tricuspid annular motion velocity.

Fig. 4. Bland-Altman analyses between interobserver measurements of the five

echocardiographic parameters

Solid lines on Bland-Altman plots indicate mean differences; dashed lines indicate limits of agreement. %RVFS, right ventricular fractional shortening; TAPSE, tricuspid annular plane systolic excursion; RV MPI, right ventricular myocardial performance index; TV_{lat} , systolic lateral tricuspid annular motion velocity.

Figure 1

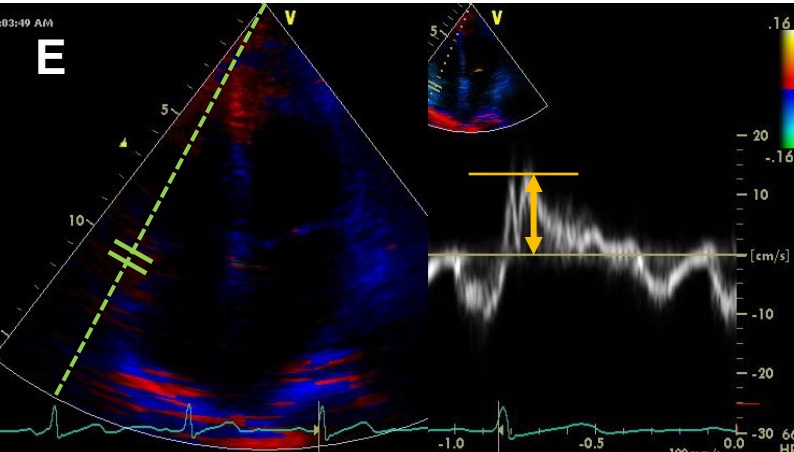
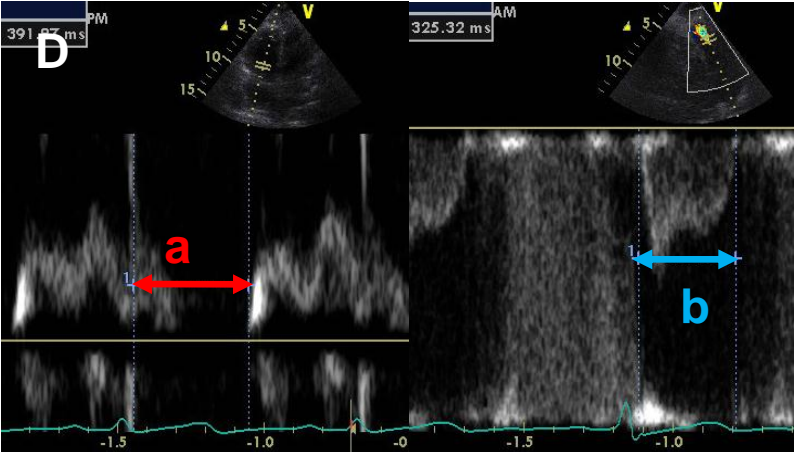
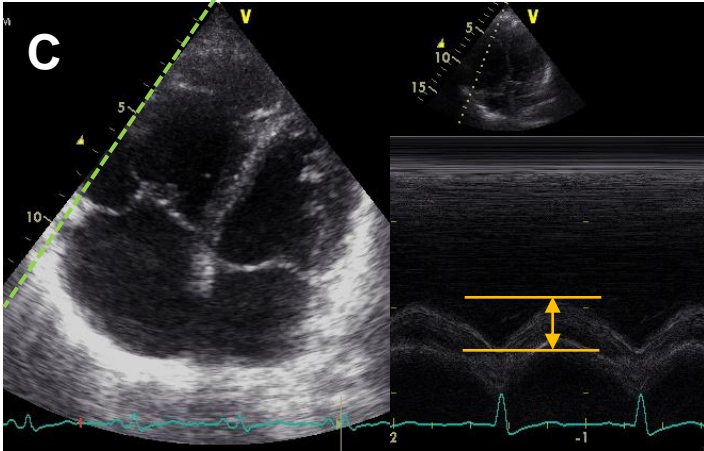
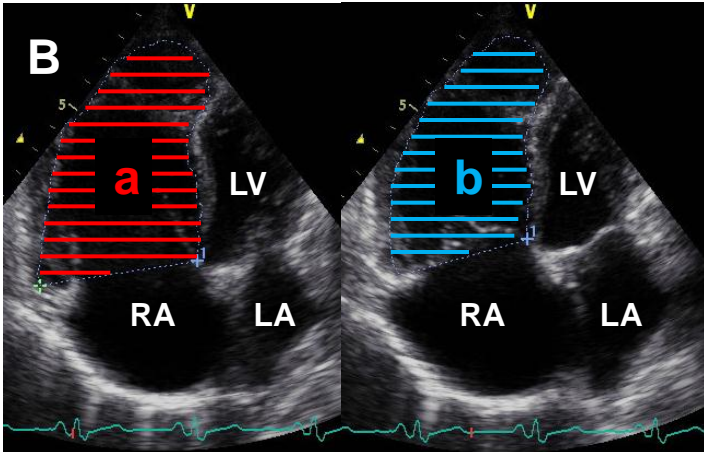
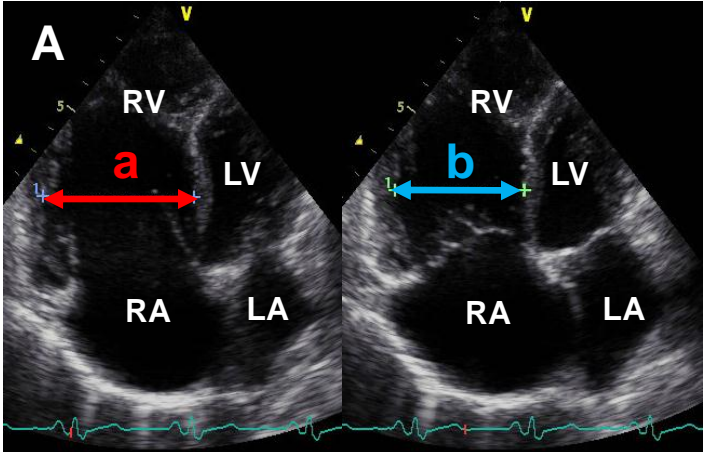
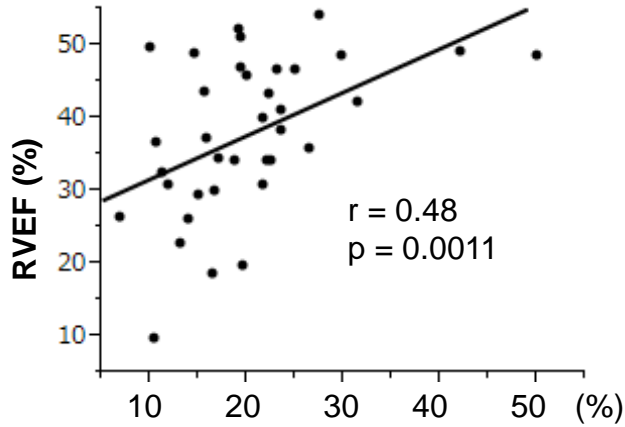
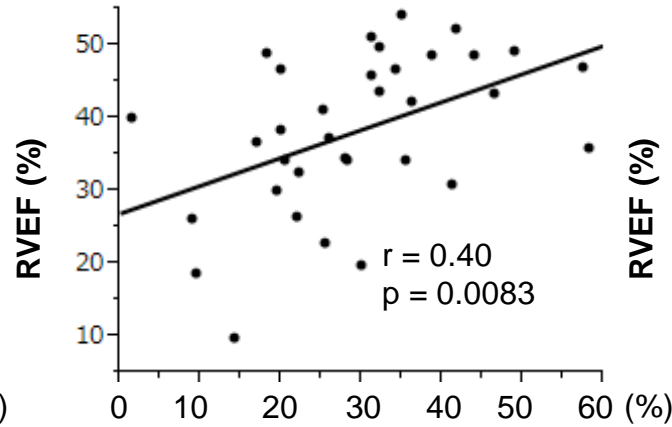


Figure 2

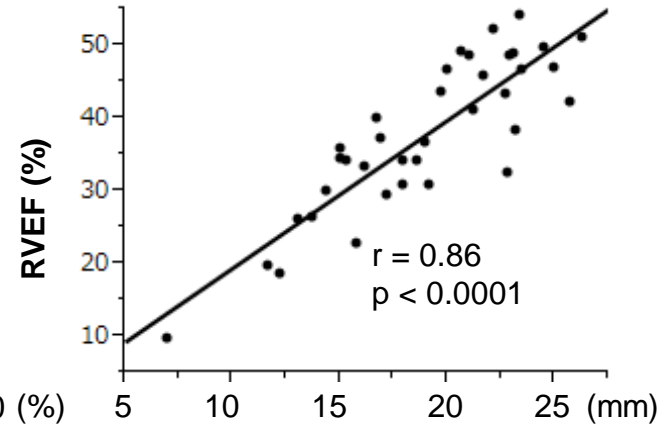
%RVFS



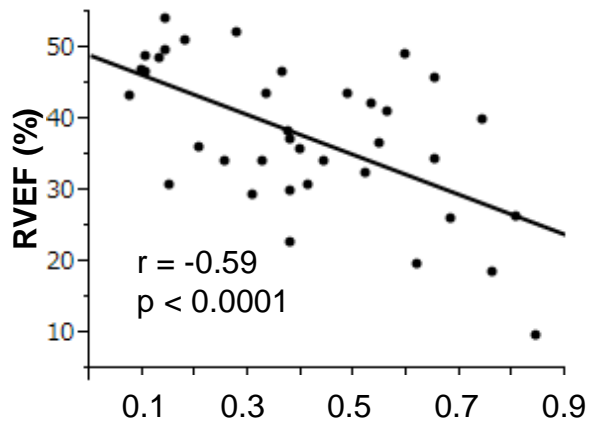
%RV area change



TAPSE



RV MPI



TV_{lat}

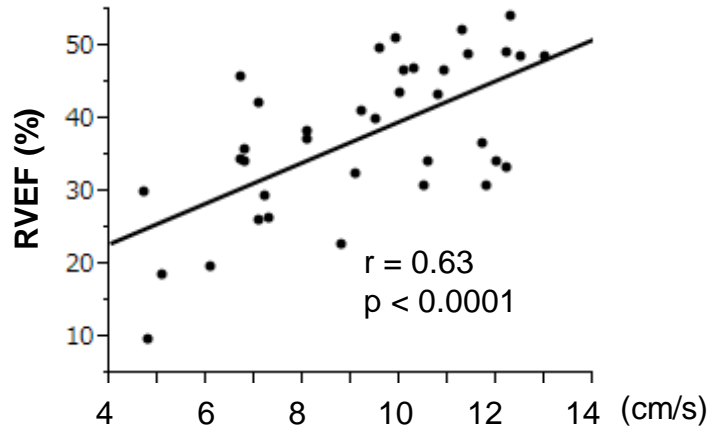


Figure 3

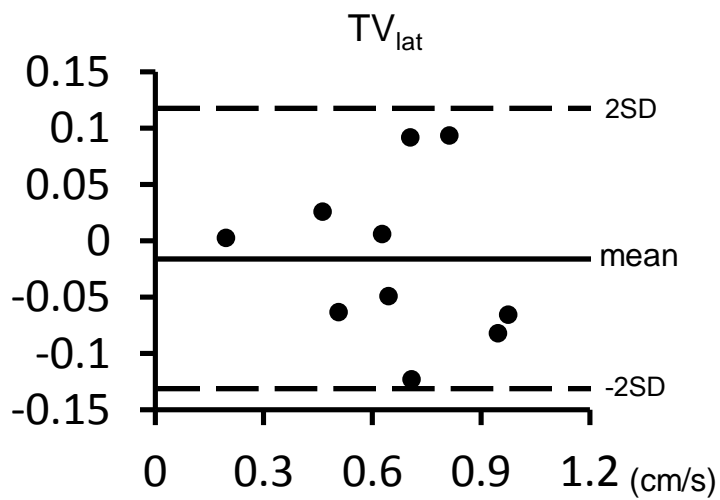
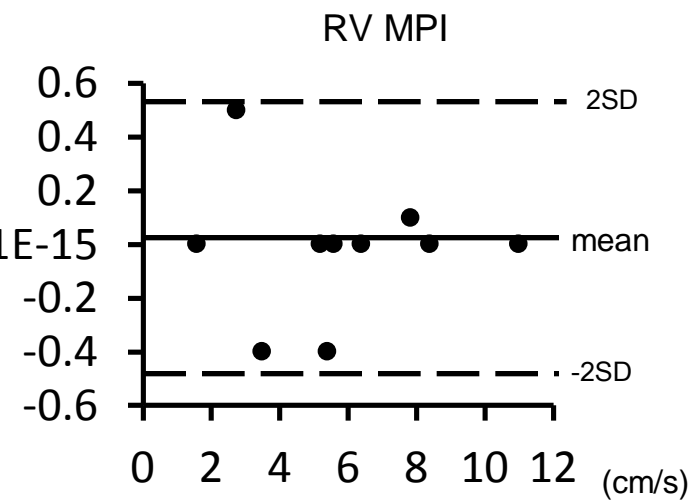
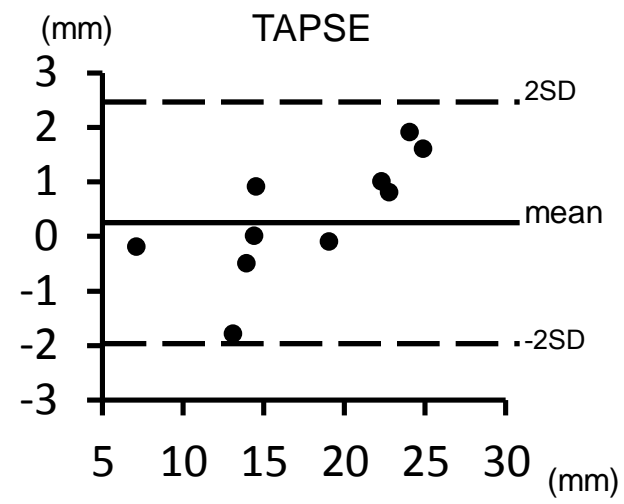
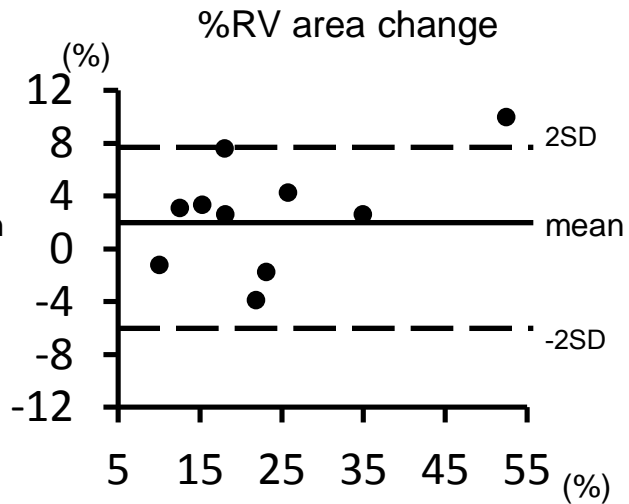
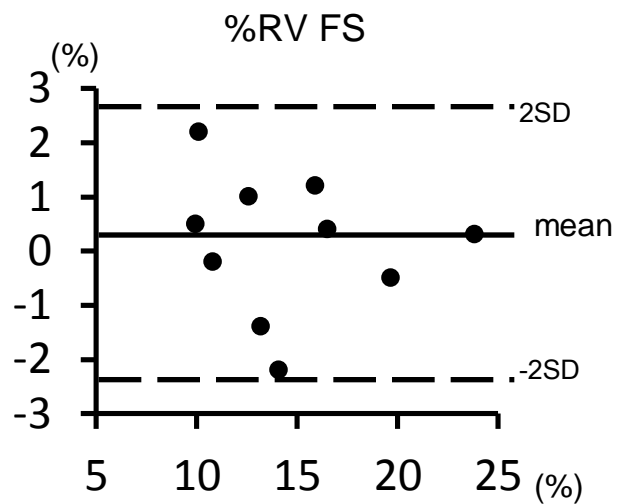
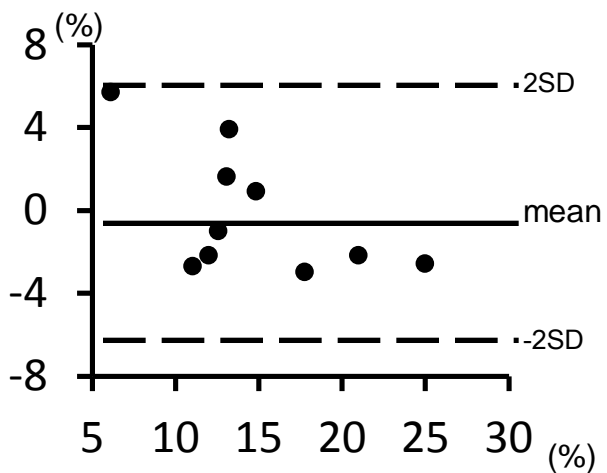
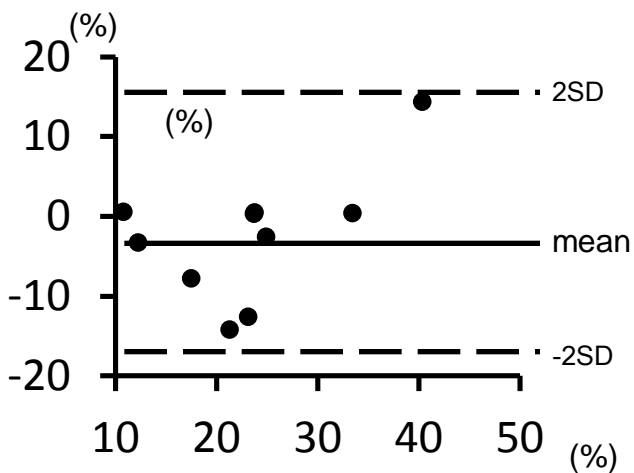


Figure 4

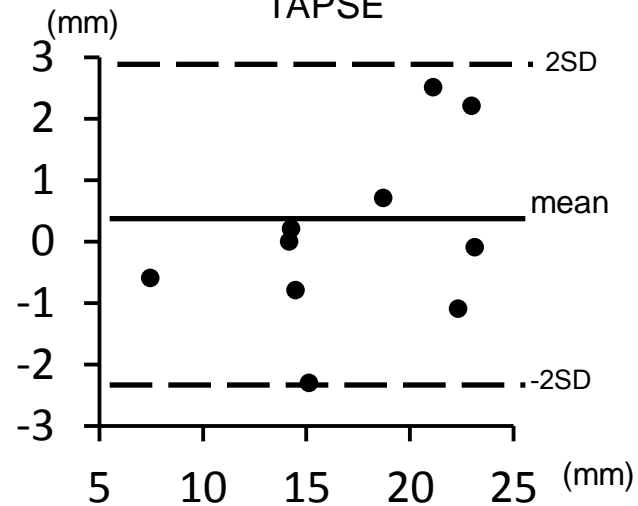
%RV FS



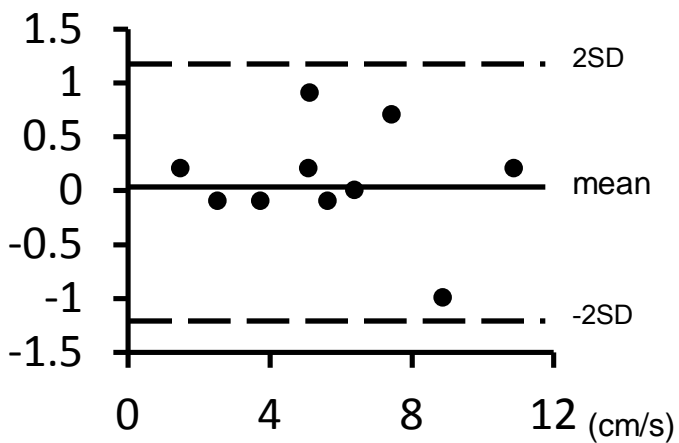
%RV area change



TAPSE



RV MPI



TV_{lat}

